Available online at www.sciencedirect.com
SCIENCE DIRECT
Catalysis Today 109 (2005) 104–111
CATALYSIS TODAY
www.elsevier.com/locate/cattod

Hydroconversion kinetics of Marlim vacuum residue

Rafael Menegassi de Almeida [a,*], Reginaldo Guirardello [b]

[a] Petrobras Research Center—CENPES, Brazil
[b] School of Chemical Engineering, State University of Campinas—UNICAMP, Brazil

Available online 3 October 2005

Abstract

A kinetic model was obtained for the Marlim crude vacuum residue (VR) hydroconversion. Marlim VR mixed with FCC decant oil in an 80%/20% weight basis was put in contact with a commercial NiMo on γ-alumina catalyst in a stirred batch reactor. Several temperatures and oil/catalyst ratios were used over different times (0–240 min), at a 110 bar pressure and constant hydrogen flow. The analysis of the collected product showed residua conversions of up to 70%. Hydroconversion kinetics involving thermal and catalytic cracking contributions was proposed to represent the obtained data. The resulting system of differential equations of the kinetic model was solved within reaction time, taking into account the experimental temperature profile. The chi-square objective function was minimized to adjust model parameters. A proposed effective hybrid minimization method was used, by applying a Newton-type method between certain simulated annealing minimization steps. The proposed kinetic model allowed the representation of thermal and catalytic cracking effects, in order to take into account different catalyst concentrations. Therefore it is possible to consider distinct reactor hydrodynamics, such as expanded or bubble column reactors.

Keywords: Marlim vacuum residue; γ-Alumina; Newton-type method

1. Introduction

The oil refining scenario can be described as an increase in heavy oil and natural gas production, and a higher demand for better quality distillate products. Hydroconversion of vacuum residues (VR) is the preferred method for bottom of the barrel conversion when maximum diesel oil yield is desired. Hydroconversion consists of putting the VR in contact with hydrogen in the presence of a catalyst. The operational conditions range from fixed or moving bed to ebullated or expanded-bed and slurry reactor. Large pore NiMo alumina-supported catalysts are preferred for this application. Catalyst holdup at hydroconversion is reported as ranging from 5% to 40% in volume [1,2].

Kinetics of VR hydroconversion are usually obtained in fixed bed, with the highest catalyst holdup, or using catalyst as an additive (low catalyst holdup). Under these conditions, the kinetics are expressed either as a function of catalyst quantity or reactor volume. In practice, catalyst holdup in an ebullated-bed reactor remains between the two cited limits, having both thermal and catalytic contributions to conversion and other reactions.

In spite of the industrial importance, there are not many published kinetics taking into account the effect of catalyst concentration. As an example, the inclusion of an adjusted-power catalyst concentration term multiplied by the mass action law kinetics can be cited [3]. It is related to the development of the LC-Fining process.

Hydroconversion kinetic data is commonly obtained in continuous reactors. Batch reactors have the disadvantage of a heating period, being difficult to define the start of reaction, which leads to the development of methods such as the time elimination procedure or the fitting of an additional parameter describing the lapse between the start of the reaction and the first measure [4]. Some authors do not consider the heating period [5]. Other procedures that take this into account are the equivalent residence time [6] and the integration of a first-order reaction rate accounting for a constant heating rate [7]. Both procedures are difficult to apply to more complex kinetic models. It is considered difficult to calculate rate constants from non-isothermal data of complex reaction systems, with multiple reactions of different activation energies. The difficulty arises from the existence of many local minima in the least squares function minimization [8]. On the other hand, parameters fitted

* Corresponding author.
E-mail addresses: menegassi@petrobras.com.br (R.M. de Almeida), guira@feq.unicamp.br (R. Guirardello).

0920-5861/$ – see front matter © 2005 Elsevier B.V. All rights reserved.
doi:10.1016/j.cattod.2005.08.021

using non-isothermal data are considered to be more representative [9].

In this work, procedures are proposed to: utilize non-isothermal batch reactor for obtaining vacuum residue hydroconversion kinetic data; have improved curve fitting procedure and obtaining kinetic models for hydroconversion that could be used for simulation of different reactor types (fixed, ebullated, slurry bed reactors) [10].

2. Experimental

Marlim is a low-sulfur high nitrogen content 20 API heavy crude. A Marlim crude vacuum residue mixed with FCC decant oil in the proportion of 80–20 wt% was used as feedstock. Decant oil is useful to prevent dry sludge formation, allowing higher residue conversions. The resulting feedstock had a density of 4.55 API, with sulfur, nitrogen and vanadium contents of 9600, 10,000 and 69 ppm, respectively. TLC-FID SARA analysis of the feedstock showed 4 wt% saturated, 27 wt% aromatics, 36 wt% resins and 33 wt% asphaltenes. Elemental analysis of the feedstock showed 87.63% carbon, 9.43% hydrogen and 1.02% nitrogen. More data on Marlim VR can be found elsewhere [11], including discussion of the effect of decant oil on slurry hydrocracking [12].

A quantity of 400 g of feedstock was added to a 1 l Parr autoclave stirred reactor. A commercial HDM NiMo supported in γ-Al_2O_3 catalyst was ground to $-42 + 100$ mesh Tyler granulometry. Catalyst metal content was 1.5% Ni and 8% Mo supported on alumina and textural properties were 150 m^2/g BET area and 0.66 m^3/g pore volume. The catalyst was added to the reactor at three different levels: 20, 40 and 80 g—an oil/cat ratio of 20, 10 and 5 g/g, respectively.

Hydrogen control and auxiliary systems were added to the Parr autoclave, including a high and low-pressure separator and an inline filter used during reactor depressurization and product collection. The reactor set-up was previously used to test hydroconversion catalysts [13].

A pressure control valve was employed to keep the reactor pressure constant, with a controlled purge of hydrogen and product gases. The added hydrogen flux was 2 NL/min, in order to be compatible with typical industrial gas/feedstock recycle gas ratios. The reactor pressure was kept constant at 110 bar. Small quantities (less than 20 g) of distillate compounds were collected in a high-pressure trap after reactor depressurization and added to the main liquid product prior to analysis.

Other conditions were reaction times of 0, 30, 60, 120 and 240 min after the main temperature was achieved, with temperatures at T_{BASE}, $T_{BASE} - 15$ °C, $T_{BASE} + 15$ °C and $T_{BASE} + 30$ °C. A 60 min previous set-point temperature level was established at $T_{BASE} - 35$ °C in order to allow the catalyst to be fully sulfided and active prior to achieving the higher desired temperatures, at which coke deposition would be less gentle. It was believed that such a procedure would ensure more representative data, as the catalyst would achieve higher temperature with alumina acidity previously coked at lower temperature. Upon reaction completion, the reactor was quenched with water coils and depressurized. Catalyst and liquid product were separated in an inline +150 mesh Tyler filter directly connected to the bottom of the reactor, and both weighted. At the end of each run, the reactor was opened and small quantities of uncollected slurry product (less than 10 g) were carefully weighted.

Table 1
Reaction conditions

Run number	Reaction temperature set-point (°C)	Time after reaching temperature (min)	Oil/cat (w/w)
1	T_{BASE}	0	10
2	T_{BASE}	30	10
3	T_{BASE}	60	10
4	T_{BASE}	120	10
5	T_{BASE}	120	5
6	$T_{BASE} + 15$	120	10
7	T_{BASE}	240	10
8	T_{BASE}	120	20
9	$T_{BASE} - 15$	120	10
10	$T_{BASE} - 15$	60	10
11	$T_{BASE} + 15$	60	10
14	$T_{BASE} + 30$	60	10

The test conditions are presented in Table 1. During each test, the temperature along run time was recorded. The temperature profile of each test is presented in Fig. 1. The second temperature level from now on is called the reaction temperature. This reaction temperature is also presented as the difference from the base temperature (T_{BASE}) that was used for reparametrization. It can be seen that the heating times and the previous 60 min lower temperature step are significant.

Both the feedstock and products were analyzed for extended simulated distillation (ASTM D5307) and microcarbon residue (ASTM D4530). Sulfur and vanadium contents were also measured in the products, but reported elsewhere [14,15]. Simulated distillation data was used to calculate the yield of the desired product lumps (naphtha + gas, diesel, gasoil and residue). Naphtha + gas were considered as IBP-180 °C, diesel as 180–380 °C, gasoil as 380–540 °C and residue >540 °C. Gas and naphtha lump was considered as the sum of simulated distillation 180 °C—plus the mass balance difference. Micro-

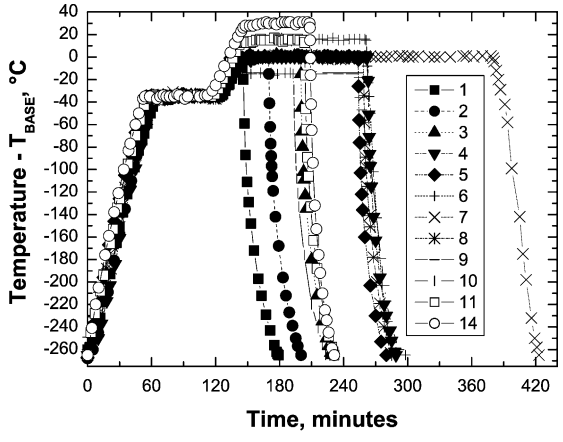

Fig. 1. Reactor temperature profiles of experimental runs 1–11 and 14.

Table 2
Feedstock and products mass fractions and liquid product yield

Run	Liquid yield (wt%)	Naphtha + gas (IBP 180 °C)	Diesel (180–380 °C)	Gasoil (380–540 °C)	Residue (>540 °C)	MCR (wt%)
Feed	–	0.000	0.091	0.123	0.786	19.2
1	99.4	0.010	0.117	0.207	0.666	16.8
2	98.6	0.016	0.148	0.222	0.615	15.6
3	98.0	0.031	0.172	0.243	0.554	15
4	97.0	0.066	0.250	0.295	0.389	13.6
5	96.3	0.051	0.252	0.276	0.421	13.1
6	96.8	0.062	0.353	0.329	0.256	11.6
7	94.5	0.069	0.287	0.291	0.353	11.2
8	97.2	0.038	0.217	0.283	0.462	14.2
9	97.7	0.034	0.152	0.261	0.553	15
10	99.0	0.012	0.130	0.259	0.600	15.9
11	97.0	0.053	0.268	0.282	0.397	13
14	94.1	0.078	0.365	0.309	0.248	14.3

carbon residue (MCR) was recalculated from the mass balance. This was considered as a small dilution effect on the MCR, assuming that the mass balance difference (considered volatiles) had zero MCR, and adding this to the liquid product, diluting the original MCR value.

Two other runs with a slightly different HDM catalyst, not used in the present kinetics, were performed to verify the tests repeatability. Conditions were pressure of 110 bar, oil/cat of 10 (w/w) and temperature of T_{BASE} + 5 °C. The product MCR was 11.8 wt% for both of the two runs; residua fraction were 0.449 and 0.440, gasoil fractions were 0.551 and 0.560, diesel fractions were 0.276 and 0.282 and naphtha + gas fractions were 0.025 and 0.034. The relative error was very small, about 2% for diesel, gasoil and residua, comparatively higher for naphtha and gas (34%), although small in absolute value (0.88%). The higher error in the naphtha and gas is expected, as it is calculated from both the mass balance and analysis. Other ways of improving the balance would mean continuous analysis of gaseous effluent, analysis of spent catalyst and quantity of hydrogen added to the products.

There were 12 experiments, with 5 lumps (4 independent), totaling 60 experimental data points (48 independent, as the sum of fractions is equal to 1).

Characteristics of the feedstock and products are presented in Table 2. Results are also plotted in Figs. 2–5.

It can be seen in Fig. 2 that an increase in reaction time results in a higher conversion of the vacuum residue to other desired fractions, gasoil, diesel and naphtha.

Fig. 3 presents the 120-min runs results at different reaction temperatures. The temperature increase resulted in a higher VR fraction conversion, to mainly the diesel oil fraction, and, to a lower extent, gasoil and naphtha + gas fractions.

Fig. 4 presents the results of the microcarbon residue (MCR) content in the liquid product. It can be seen that conversions were higher as the time increased. Higher temperatures led to higher MCR conversions. Increase in catalyst mass present in the reactor (from oil/cat = 10 g/g to oil/cat = 5 g/g) also resulted in higher MCR conversion, and lower catalyst content (oil/cat = 20 g/g) lowered the conversion.

Regarding the effect of catalyst quantity on product distribution, Fig. 5, a catalyst increase led to a tendency of higher vacuum residue conversion, lower gasoil and higher diesel oil content. Compared to the catalytic effect on HDS and HDM reactions [14,15], the effect in conversion is lower, but should not be disregarded. In spite of the lower effect on conversion, the catalyst plays an important role in stabilization of thermal cracking radical moieties. Also, hydrogenation of the aromatic cores makes it easier to crack the feed into lower boiling point compounds.

3. Data fitting

One of the main goals of this work was to use the batch data to develop a kinetic model that further represents the hydroconversion of Marlim vacuum residue.

The batch reactor model plus the proposed kinetic result in a set of ordinary differential equations (ODEs). The ODES were solved by the LSODA code [16]. During the ODEs solving, the temperatures at each integration time step were calculated by interpolation of the data presented in Fig. 1. On this basis, the temperature changes in the reactor were fully taken into account.

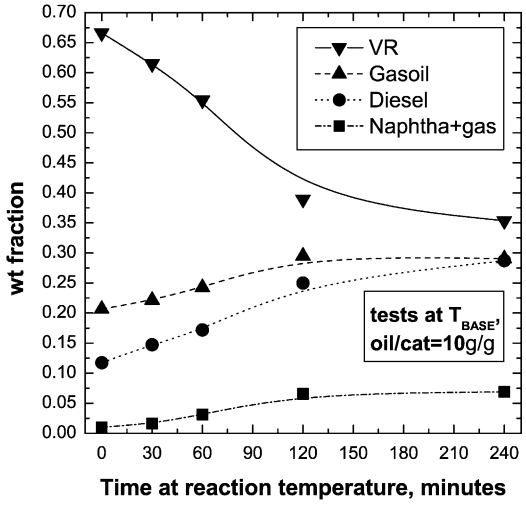

Fig. 2. Effect of time on experimental product composition, at base temperature and oil/cat = 10 (w/w).

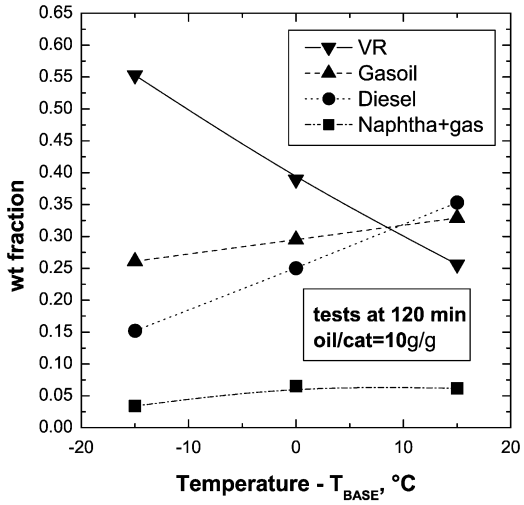

Fig. 3. Effect of temperature on experimental product composition, at 2 h time and oil/cat = 10 (w/w).

It can be seen in Table 2 that for the time zero after reaching reaction temperature, run number 1, there has been significant conversion of residue and MCR resulting from the heating profile. It should be emphasized that the feedstock data used for fitting is the real feedstock, as the temperature profiles were taken into account, and not the ''time zero'' result of run 1. The procedure of taking into account the temperature heating profile can eliminate the problem of defining the initial reaction time for such experiments.

With the kinetic model defined and implemented, a suitable representation of the difference of calculated and experimental (chi-square function) was minimized using a proper method.

3.1. Reactor and kinetic models

Residue conversion is considered to be mainly thermal, but a catalytic effect could be seen from the data. To take into account the catalyst effect, thermal and catalytic reactions were considered in parallel. This is in fact not true, as the catalyst hydrogenation function is involved in stabilization of thermal

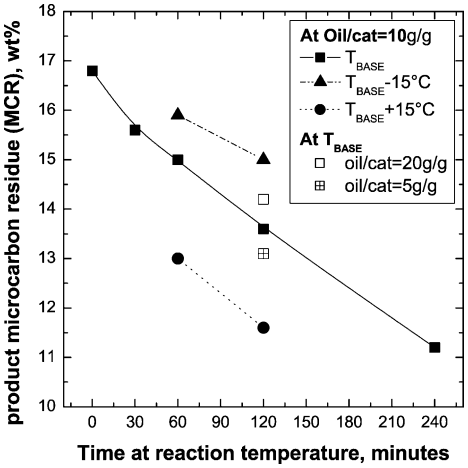

Fig. 4. Effect of time, temperature and oil/cat on experimental product microcarbon residue (MCR).

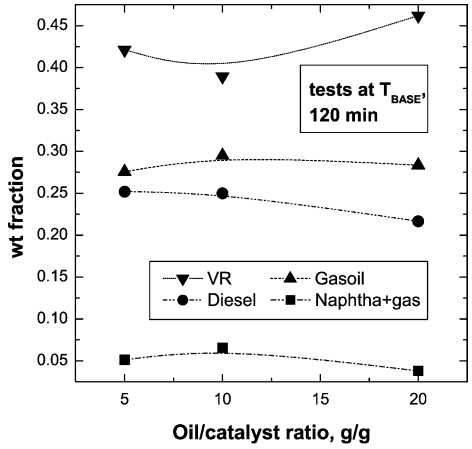

Fig. 5. Effect of oil/cat ratio on experimental product composition, at T_{BASE} and 2 h reaction time.

cracking intermediate products, and the reactions are not uncoupled [17,18]. On the other hand, it is a convenient way to express the effect of catalyst without addition of a catalyst concentration power constant. The catalytic reactions are related to the quantity of catalyst in the reactor, and the thermal reactions are related only to the reactant concentration.

Also, it was assumed that the VR (>540 °C) could be represented by easy and hard portions. The hard residue is represented by the microcarbon assay value (MCR) and the easy residue (VReasy) corresponds to the difference of >540 °C residue and the MCR. Therefore, VReasy = VR − MCR. The total residue (>540 °C) is thus represented by the sum of easy and hard portions, VReasy and MCR respectively. It is assumed that each portion has different kinetics. This procedure allowed better representation of the existence of more and less refractory residue molecules. It is a reasonable assumption, as most of the material that results in carbonaceous products during coking (MCR) is present in the residue. The MCR portion is directly related to the polyaromatic portion of molecules, and the VReasy related to naphthenic, paraffinic and smaller aromatic moieties attached to those polyaromatic cores.

The considered reactions are presented on Fig. 6. The reactions between MCR and VReasy were considered to be reversible, in order to represent the complex chemistry of residuum conversion, during which dehydrogenation and coking could also occur. Both thermal and catalytic reactions were considered to occur in parallel. All other reactions are irreversible. Thermal and catalytic reaction of gasoil to diesel and naphtha + gas can be expected to some extent, as thermal cracking and some hydrogenolysis can take place, and even some shift in the boiling point due to hydrogenation (catalytic). Further cracking of diesel to naphtha and gas is not expected (lower boiling point hydrocarbons tend to be more thermally stable), nor the catalytic conversion of gasoil to naphtha + gas (boiling change shift would not be so significant).

In order to minimize the number of parameters to be fitted, the equivalent activation energies of reactions 7, 8, 10, 11, 12 and 13 are assumed to be equal to those of reactions 6, 1, 2, 3, 4 and 9, respectively. This simplification is necessary since the catalyst mass variation tests were held at just one reaction

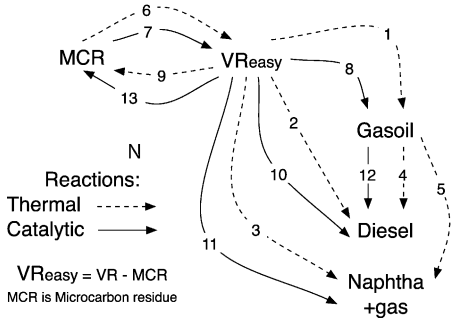

Fig. 6. Reaction network for hydroconversion.

temperature. There is not sufficient data to fit different activation energies. More data with different catalyst concentration at several temperatures would be necessary. It means therefore that a convenient way of expressing the effect of catalyst quantity, retaining some chemical meaning—different from the addition of a catalyst concentration term to a power, as suggested elsewhere [3].

The considered reactions lead to the following set of ordinary differential equations:

$$\begin{aligned}
\frac{d\eta_{VReasy}}{dt} &= +r_6 + r_7 - r_1 - r_2 - r_3 - r_8 - r_9 - r_{10} - r_{11} - r_{13} \\
\frac{d\eta_{MCR}}{dt} &= -r_6 - r_7 + r_9 + r_{13} \\
\frac{d\eta_{Gasoil}}{dt} &= +r_1 + r_8 - r_4 - r_5 - r_{12} \\
\frac{d\eta_{Diesel}}{dt} &= +r_2 + r_4 + r_{10} + r_{12} \\
\frac{d\eta_{Naphtha+gas}}{dt} &= +r_3 + r_5 + r_{11}
\end{aligned} \tag{1}$$

where t is time (min), r reaction rate and η_i is the response of lump i (mass fractions).

Thermal reaction rates are expressed as pseudo first-order kinetics:

$$\begin{aligned}
r_1 &= k_1 \cdot \eta_{VReasy} \\
r_2 &= k_2 \cdot \eta_{VReasy} \\
r_3 &= k_3 \cdot \eta_{VReasy} \\
r_4 &= k_4 \cdot \eta_{Gasoil} \\
r_5 &= k_5 \cdot \eta_{Gasoil} \\
r_6 &= k_6 \cdot \eta_{MCR} \\
r_9 &= k_9 \cdot \eta_{VReasy}
\end{aligned} \tag{2}$$

and the catalytic reaction rates are expressed as:

$$\begin{aligned}
r_7 &= k_7 \cdot \eta_{MCR} \cdot M_{Cat} \\
r_8 &= k_8 \cdot \eta_{VReasy} \cdot M_{Cat} \\
r_{10} &= k_{10} \cdot \eta_{VReasy} \cdot M_{Cat} \\
r_{11} &= k_{11} \cdot \eta_{VReasy} \cdot M_{Cat} \\
r_{12} &= k_{12} \cdot \eta_{Gasoil} \cdot M_{Cat} \\
r_{13} &= k_{13} \cdot \eta_{VReasy} \cdot M_{Cat}
\end{aligned} \tag{3}$$

where M_{Cat} is the mass of catalyst divided by the mass of feedstock added to the reactor (cat/oil ratio).

The reaction rate coefficients, k_i, are expressed according to the Arrhenius equation and reparametrized kinetic constants:

$$k_i = \exp\left[K_i - \sqrt{(E_i)^2}10^4\left(\frac{1}{T} - \frac{1}{T_{BASE}}\right)\right] \tag{4}$$

where T is temperature, in K; T_{BASE} is the base temperature (K); K_i and E_i are reparametrized constants to be fitted, respectively, equivalent to a pre-exponential factor and an activation energy divided by the gas constant. The reparametrization makes the data fitting procedure easier, eliminating constraints and reducing correlations between the parameters [19,20]. The proposed kinetic model, Eqs. (1)–(4), has a total number of 20 parameters. The use of pseudo first-order reactions is quite usual in lumped kinetics of heavy hydrocarbon conversion [5].

Several kinetic models were proposed and tested elsewhere [15]. The presented model can be considered a reasonable compromise between the number of parameters and the fitting result.

3.2. Minimization method

The sum of the square of the differences between the calculated and simulated responses (chi-square function) was minimized. It was difficult to compare the ability of different models to fit the data using constants obtained with local minimization methods [15]. The lack of fit of a model could be due to a bad initial approximation of the parameters and insufficient parameter fitting.

A hybrid global method was proposed. The hybrid method consists of a combination of a simulated annealing implementation of the Nelder and Mead Simplex method [21] and a local minimization Newton-type method for general unconstrained minimization [22].

In the global optimization simulated annealing method a ‘‘temperature’’ parameter ensures a random characteristic to the minimization steps, sometimes going uphill, allowing escape from local minima. A group of function minimizations (Nelder and Mead Simplex) are performed at each ‘‘temperature’’. As the annealing proceeds, the ‘‘temperature’’ lowers, and less probable become uphill steps, and the method turns equivalent to the usual Simplex. The hybrid procedure consists of performing a local Newton-type minimization at each simulated annealing ‘‘temperature’’ decrease step. The initial parameter values fed to the Newton-type method are the best parameters of that particular simulated annealing ‘‘temperature’’ step. The new local minimum is then added to the simplex, and a new simulated annealing step performed.

The proposed method, in spite of higher number of function calculations compared to the conventional Newton-type method, allowed escaping from many local minima, and effectively reaching other local minima (Newton-type step) faster. Although there is no warranty of global minima [21], it prevented from using the somewhat tedious and arbitrary

procedure of running the fitting process with several different initial parameter estimates. The existence of many local minima could be seen from the change of chi-square values along the fitting procedure [15]. After establishing sufficient annealing temperature decay and performing the minimization, results were considered to be at least sufficiently good to be comparable to other fittings using the same procedure. Different kinetic models could thus be compared, being presented elsewhere [15].

The Newton-type method needs an estimate of the gradient vector and the Hessian matrix of the chi-square function to the parameters. Both the gradient and the Hessian were calculated through the sensitivity coefficients [23]. To calculate the sensitivity coefficients additional differential equations are solved along time [24]. The precision of the gradient and Hessian thus obtained is as good as that obtained in the solution of the ODEs, and significantly better than numerical derivatives.

3.3. Fitting results

The fitting results of the proposed hydroconversion kinetic model are presented in Fig. 7 and Table 4. The data fitting is good for all considered lumps. The fit is particularly good for diesel and MCR.

The obtained kinetic parameters are presented in Table 3.

A comparison of the relative kinetic constants at different temperatures is presented in Table 4. The kinetic constants were divided by the kinetic constant of reaction 1 at T_{BASE}. When the reaction is catalytic, it is further multiplied by the mass of catalyst per unit mass of feedstock, 0.1 (assuming oil/cat ratio of 10).

It can be seen that the rate of conversion of VReasy fraction to gasoil (reaction 1) is highest at T_{BASE}, followed by the conversion of the MCR fractions to VReasy (reaction 6) and the thermal hydrocracking of the VReasy to diesel (reaction 2). As the temperature increases, the direct conversion of VR to diesel becomes more important. The rates of MCR to VReasy

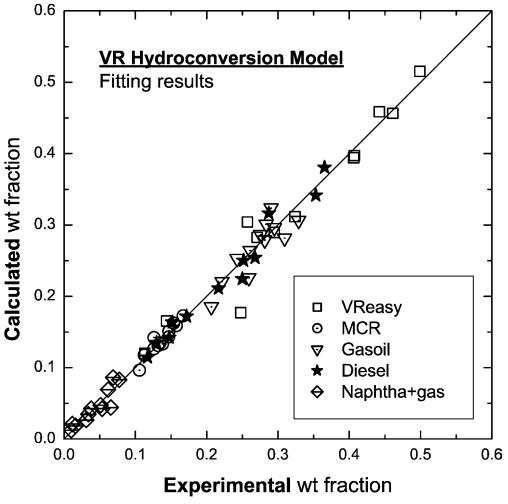

Fig. 7. Fitting result: model calculated vs. experimental data.

Table 3
Fitted parameters of the proposed kinetic model

Reaction	Parameter		Parameter	
1	K_1	−5.6540E+0	E_1	1.1439E+0
2	K_2	−6.6008E+0	E_2	3.4269E+0
3	K_3	−1.0990E+1	E_3	5.6135E+0
4	K_4	−7.2361E+0	E_4	3.8051E−1
5	K_5	−6.9977E+0	E_5	3.7586E−1
6	K_6	−6.0889E+0	E_6	1.1762E+0
7	K_7	−6.0410E+0	E_7	$=E_6$
8	K_8	−8.4719E+0	E_8	$=E_1$
9	K_9	−9.8186E+0	E_9	4.7179E+0
10	K_{10}	−5.6081E+0	E_{10}	$=E_2$
11	K_{11}	−7.0947E+0	E_{11}	$=E_3$
12	K_{12}	−6.1725E+0	E_{12}	$=E_4$
13	K_{13}	−9.5203E+0	E_{13}	$=E_9$

(reactions 6 and 7) are bigger than the reverse kinetic constants (reactions 9 and 13). The thermal conversion of gasoil to diesel is favored at higher temperatures, but it is smaller than the direct conversion of VReasy lump to the diesel. Further, the separation of VR in a hardly converted portion (MCR is a direct measure of the coking at high temperature) and the easy VR allowed previewing both the MCR product and the final VR conversion. Concerning the cracking of higher boiling products to naphtha and gas, more experimental data would be necessary to better separate thermal and catalytic effects of VR conversion to naphtha and gas (reactions 3 and 11). On the other hand, catalyst alumina acidity can play some role in favoring cracking.

It is not the objective of this study to clarify the hydrocracking mechanisms through kinetic analysis. The model proposed and the relative fitted constants represent well the experimental data. The model results agree with previously discussed pathways on residue conversion. According to Sanford [17,18] most of the distillate and gas come directly from common radical precursors formed by thermal activation of labile chemical bonds of the residue molecules. For example, in the relative rate constants presented on Table 5, the direct reaction pathway to diesel formation, reactions 2 and 10, have higher values than the gasoil to diesel reactions 4 and 12.

4. Simulations

The obtained hydroconversion kinetics was used to simulate products at fixed temperatures, reaction times, and oil/cat ratios. Some of the conditions were beyond the range employed experimentally. Simulation results are presented in Figs. 8–10. Total residue VR fraction, the MCR and the difference of both (VReasy) are presented. It is important to notice that constant reaction temperatures were assumed during each simulation period. It is also a way to preview the results that would be obtained without the heating profile.

In Fig. 8, at the temperature of $T_{BASE} + 30\ ^{\circ}C$ and oil/cat = 10 (w/w) the reaction time was increased. It can be seen that MCR is much more difficult to convert than the easy portion. The easier portion of VR is almost completely cracked at 240 min. Gasoil fraction in the product attains a maximum at

Table 4
Calculated values vs. experimental data, fraction of MCR, VReasy, gasoil, diesel and naphtha + gas

Test	MCR		VReasy		Gasoil		Diesel		Naphtha + gas	
	calc	exp	calc	exp	calc	exp	calc	exp	calc	exp
1	0.17263	0.16699	0.51539	0.4992	0.18523	0.20661	0.11447	0.1172	0.01229	0.01
2	0.16231	0.15382	0.45648	0.46093	0.22059	0.22165	0.14216	0.14751	0.01846	0.01609
3	0.15107	0.147	0.39738	0.40721	0.25291	0.24274	0.17192	0.17189	0.02671	0.03117
4	0.13113	0.13192	0.3043	0.25736	0.29609	0.29509	0.22437	0.25006	0.04411	0.06556
5	0.12648	0.12609	0.28952	0.29507	0.28642	0.27565	0.25014	0.25194	0.04744	0.05125
6	0.11756	0.11231	0.16543	0.14374	0.30626	0.32898	0.3416	0.35324	0.06915	0.06173
7	0.09638	0.10589	0.17716	0.24755	0.32368	0.29055	0.31651	0.28711	0.08626	0.0689
8	0.13338	0.13802	0.31161	0.32386	0.30113	0.28349	0.21131	0.2166	0.04257	0.03803
9	0.14324	0.14659	0.39427	0.40623	0.26405	0.26102	0.16369	0.15198	0.03475	0.03417
10	0.15906	0.15741	0.45881	0.44211	0.22605	0.25917	0.13507	0.12978	0.02101	0.01153
11	0.14228	0.12616	0.28258	0.271	0.27871	0.28158	0.25411	0.26788	0.04232	0.05338
14	0.13497	0.13455	0.11996	0.11312	0.28153	0.30944	0.38059	0.36539	0.08296	0.0775

calc: calculated; exp: experimental.

Table 5
Relative rate constants, k_i/k_1, k_1 at $T = T_{BASE}$, further multiplied by M_{Cat} if catalytic ($M_{Cat} = 0.1$)

Reaction	Nature	$T = T_{BASE}$	$T = T_{BASE} + 15$	$T = T_{BASE} + 30$
1	Thermal	1.000	1.426	2.003
2	Thermal	0.388	1.122	3.106
3	Thermal	0.005	0.027	0.145
4	Thermal	0.206	0.231	0.259
5	Thermal	0.261	0.293	0.328
6	Thermal	0.647	0.932	1.322
7	Catalytic	0.068	0.098	0.139
8	Catalytic	0.006	0.009	0.012
9	Thermal	0.016	0.067	0.272
10	Catalytic	0.105	0.303	0.838
11	Catalytic	0.024	0.135	0.715
12	Catalytic	0.060	0.067	0.075
13	Catalytic	0.002	0.009	0.037

about 100 min and diesel product keeps increasing (but naphtha and gas also increase).

In Fig. 9, temperature is varied at a fixed reaction time (120 min) and oil/cat ratio. VR conversion is more significant at temperatures higher than $T_{BASE} - 30\ ^{\circ}C$. The conversion to gasoil is more significant at $T_{BASE} + 10\ ^{\circ}C$, when the diesel becomes the more significant product. Above $T_{BASE} + 30\ ^{\circ}C$, the conversion to naphtha and gas is increased. The calculated product distribution as a function of temperature presented in Fig. 9 is very similar to data obtained for other residua feedstock [25].

The effect of the catalyst concentration on the reaction for T_{BASE} and 120 min of reaction time is presented in Fig. 10. As the catalyst concentration increases, diesel production increases.

Depending on the type of reactor and the vapor–liquid equilibrium during reaction, the more refractory residue species being retained (MCR forming), the remaining VR being easily

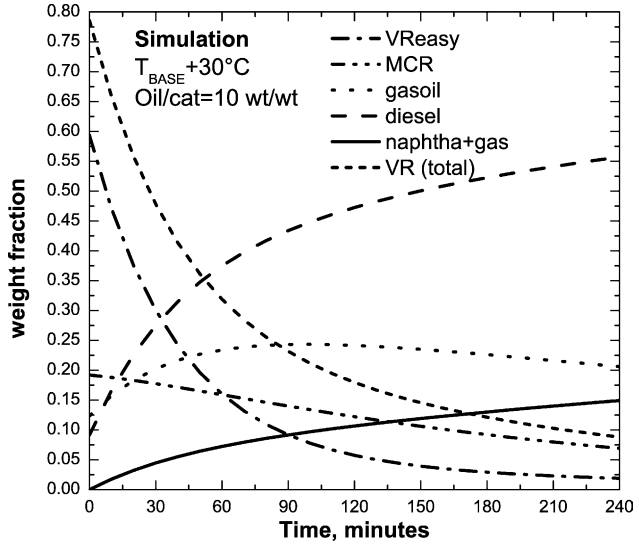

Fig. 8. Simulation results—effect of time at fixed temperature and oil/cat.

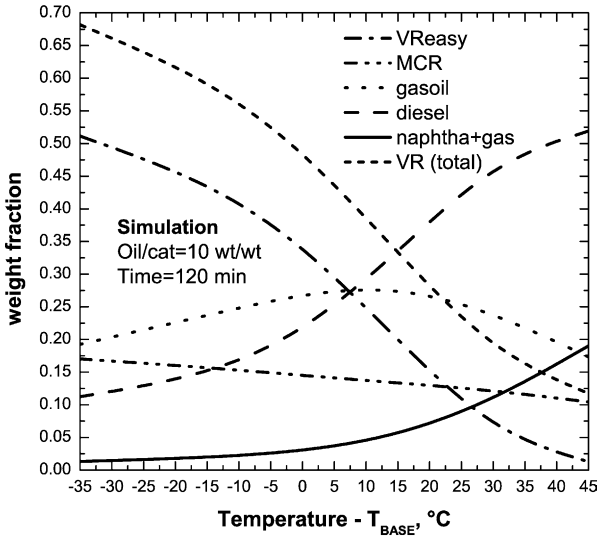

Fig. 9. Simulation results—effect of temperature at fixed time and oil/cat.

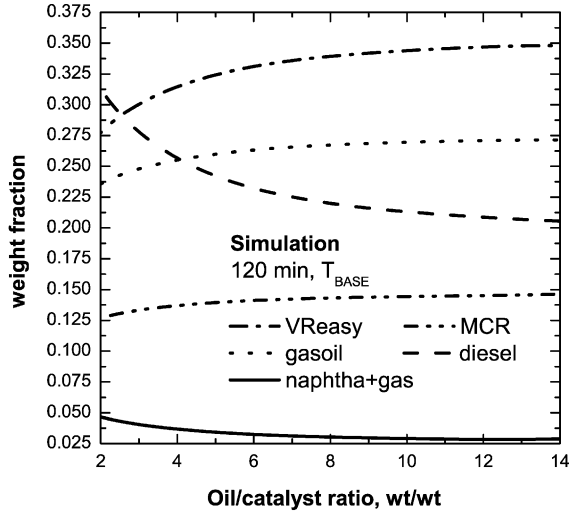

Fig. 10. Simulation results—effect of oil/cat ratio at fixed temperature and time.

converted, and the presence of naphtha (lights, mainly saturated), can lead to the precipitation of the asphaltenic micelles forming dry sludge. The dry sludge formation limits the attainable residua conversion in industrial processes. A proper optimization of a hydroconversion process scheme and conditions points to the necessity of improving the conversion of the MCR portion, maintaining its solubility.

5. Conclusions

A kinetic model representing the hydroconversion of Marlim crude vacuum residue was obtained. This was possible due to the combination of:

- procedures for obtaining experimental data in a repeatable manner in a low cost batch reactor;
- tests with different concentrations of catalyst fed to the reactor, in order to represent thermal and catalytic effects in the reactions;
- kinetic schemes able to represent the phenomena present in the vacuum residue hydroconversion;
- consideration of the temperature profile during data fitting, thus eliminating uncertainties related to the definition of the start of the reaction in non-isothermal data;
- development and use of a hybrid global convergence method for parameter estimation.

The obtained model can be further used in process scale-up and simulation using detailed reactor hydrodynamic models.

Acknowledgements

Authors would like to thank Mr. Guilherme Luís Monteiro de Souza for the fruitful discussions. Authors also thank Petrobras-Petroleo Brasileiro S.A. for permission to publish this paper.

References

[1] R. Krishna, S.T. Sie, Chem. Eng. Sci. 49 (1994) 4029.
[2] L.S. Fan, Gas–Liquid–Solid fluidization engineering, Butterworths, London, 1989, 763 pp.
[3] R.M. Eccles, Fuel Process. Technol. 35 (1993) 21.
[4] N.R. Draper, H. Kanemasu, R. Mezaki, Ind. Eng. Chem. Fundam. 8 (1969) 423.
[5] R.O. Koseoglu, C.R. Phillips, Fuel 66 (1987) 741.
[6] R.H. Heck, L.A. Rankel, F.T. Diguiseppi, Fuel Process. Technol. 30 (1992) 69.
[7] S. Kobayashi, S. Kushiyama, R. Aizawa, Y. Koinuma, K. Inoue, Y. Simizu, K. Egi, Ind. Eng. Chem. Process. Des. Dev. 26 (1987) 2241.
[8] C. Perego, S. Peratello, Catal. Today 52 (1999) 133.
[9] S. Wang, H. Hofmann, Chem. Eng. Sci. 54 (1999) 1639.
[10] M.M. Carbonell, R. Guirardello, Chem. Eng. Sci. 52 (1997) 4179.
[11] T. Kondo, S. Sato, A. Matsumura, I. Saito, A.M. Carvalho, W.F. Souza, Prepr. Symp. Am. Chem. Soc. Div. Fuel Chem. 44 (1999) 182–187.
[12] T. Kondo, H.T. Sakurai, W.F. Souza, Prepr. Symp. Am. Chem. Soc. Div. Pet. Chem. (2003) 48#3.
[13] G.L.M. Souza, H.T. Sakurai, R.M. Almeida, F.F. Rocha, G. Kaskantzis, Instituto Brasileiro de Petróleo—ARPEL Fifth Latin American Petroleum Congress/Conexpo ARPEL'96, Rio de Janeiro, October 13–17, 1996, Paper #TT-127, 8 pp.
[14] R.M. Almeida, R. Guirardello, G.L.M. Souza, Bol. Téc. PETROBRAS 42 (1999) 26.
[15] R.M. Almeida, Marlim vacuum residue hydroconversion reactions kinetics. Chemical Engineering School, Campinas State University—UNICAMP, Ph.D. Thesis, 2000.
[16] L.R. Petzold, A.C. Hindmarsh, LSODA—Livermore solver for ordinary differential equations, with automatic method switching for stiff and nonstiff problems, 24/02/97 Version, FORTRAN Subroutine, http://www.netlib.org.
[17] E.C. Sanford, Ind. Eng. Chem. Res. 33 (1994) 109.
[18] E.C. Sanford, K.H. Chung, AOSTRA J. Res. 7 (1991) 37.
[19] G. Buzzi-Ferraris, Catal. Today 52 (1999) 125.
[20] D.J. Pritchard, D.W. Bacon, Chem. Eng. Sci. 33 (1978) 1539.
[21] W.H. Press, S.A. Teukolsky, Comput. Phys. (July/August) (1991) 426.
[22] D.M. Gay, ACM Trans. Math. Software 9 (1983) 503.
[23] Y. Bard, L. Lapidus, Catal. Rev. 2 (1968) 67.
[24] V.J. Law, Y. Sharma, Comput. Chem. Eng. 21 (1997) 1471.
[25] J.F. Mosby, R.D. Buttke, J.A. Cox, C. Nikolaides, Chem. Eng. Sci. 41 (1986) 989.